UpWind

Project funded by the European Commission under the 6th (EC) RTD Framework Programme (2002- 2006) within the framework of the specific research and technological development programme "Integrating and strengthening the European Research Area"

Project UpWind.TTC

Contract No.:
019945 (SES6)

"Integrated Wind Turbine Design"

Model and numerical study of the micro damage induced anisotropy

AUTHOR:	Dr Volodymyr Kushch
AFFILIATION:	Institute for Superhard Materials NAS of Ukraine
ADDRESS:	2 Avtozavodskaya Str., 04074 Kyiv Ukraine
TEL.:	+38 044 432 9544
EMAIL:	vkushch@bigmir.net
FURTHER AUTHORS:	Sergiy V. Shmegera, Yaroslav O. Podoba, Dr Leon Mishnaevsky Jr
REVIEWER:	Project members
APPROVER:	

Document Information

DOCUMENT TYPE	Deliverable
DOCUMENT NAME:	Model and numerical study of the micro damage induced anisotropy
REVISION:	
REV.DATE:	
CLASSIFICATION:	R1: Restricted to project members
STATUS:	

Abstract: The three-level hierarchical model of micro damage induced anisotropy in the fiber reinforced composite has been developed. An early stage of fatigue damage is characterized by flaws and micro cracks formation (sub-micro level). The cyclic loading type predetermines the cracks orientation statistics which, in turn, gives rise to an anisotropy of the composite constituents. At the micro level (fiber diameter scale), the interface debonding contributes to the overall anisotropy as well because the interface cracks tend to form the chains with preferable orientation. To evaluate the damage effect on anisotropy of effective stiffness of fiber reinforced composite on each of three (sub-micro, micro and macro) level, the unified representative unit cell approach has been developed. In so doing, an actual micro geometry is modeled by a periodic structure with a unit cell containing a number of inhomogeneities sufficient to reflect the microstructure statistics The developed method combines the superposition principle, the technique of complex potentials and the new findings in the theory of special functions. An appropriate choice of potentials provides reducing the boundary-value problem to an ordinary, well-posed set of linear algebraic equations. The exact finite form expression of the effective stiffness tensor has been obtained by analytical averaging the strain and stress fields. The full-scale simulation has been performed and the statistically meaningful results obtained showing how overall stiffness reduction and damage induced anisotropy of the mechanical and conductive properties depend on angular scattering of cracks, progressive debonding and interface crack cluster formation.

Contents

STATUS, CONFIDENTIALITY AND ACCESSIBILITY										
Status				**Confidentiality**				**Accessibility**	
S0	Approved/Released			**R0**	General public			Private web site	
S1	Reviewed			**R1**	Restricted to project members	**R1**		Public web site	
S2	Pending for review			**R2**	Restricted to European. Commission			Paper copy	
S3	Draft for commends			**R3**	Restricted to WP members + PL				
S4	Under preparation			**R4**	Restricted to Task members +WPL+PL				

PL: *Project leader* **WPL:** *Work package leader* **TL:** *Task leader*

1. Sub-micro level model: effect of crack orientation statistics on effective stiffness of mircocracked solid

Publications:

1. V.I. Kushch, I. Sevostianov, L. Mishnaevsky Jr (2009) Effect of crack orientation statistics on effective stiffness of mircocracked solid. *International Journal of Solids and Structures* **46** 1574–1588

2. V.I. Kushch, S.V. Shmegera (2009) SIF statistics in micro cracked solid: Effect of crack density, orientation and clustering. *International Journal of Engineering Science* **47** 192–208

The effective elastic moduli of a micro cracked solid are rather sensitive to the density and arrangement type of cracks. Therefore, their reliable prediction requires: (a) using a geometrical model that accounts for the parameters of an actual micro structure of the cracked solid and (b) an accurate account of the crack interactions. To this end, a new, Rayleigh type method is developed providing the exact series solution for the local stress field and effective elastic properties of a cracked solid with the prescribed crack orientation statistics. The representative unit cell of a cracked solid modeled by a periodic structure contains multiple disoriented cracks of equal length, their number is taken sufficient to account for the micro structure statistics, see Fig. 1.

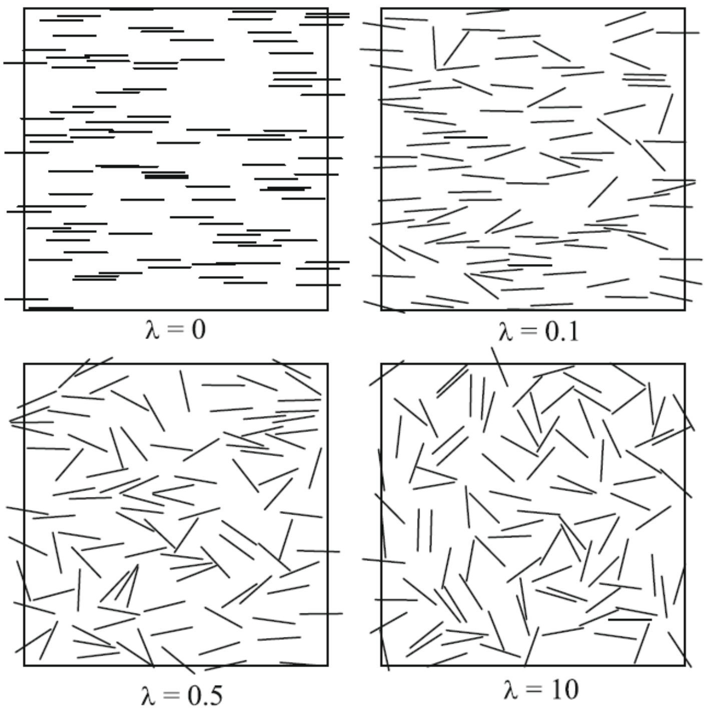

Fig. 1. Cell model of a cracked solid

The method combines the principle of superposition, technique of complex potentials and new results in the theory of special functions. A proper choice of potentials reduces the boundary-value problem to an ordinary, well-posed set of linear algebraic equations. It ensures high numerical efficiency of the developed method. The exact, finite form expressions for the components of the effective stiffness tensor have been obtained by analytical averaging of the local strain and stress fields. The exhaustive convergence study has been performed and the statistically meaningful results have been obtained showing variation of the effective elastic stiffness of cracked solid with the angular scattering of cracks.

Here, we show a few numerical data that discover an effect of crack orientation statistics on anisotropy of macroscopic stiffness of cracked solid. Table 1 contains the components C_{1313} and C_{2323} of the effective stiffness tensor of cracked solid for a series of the crack density ρ and disorder parameter λ values. As expected, $C_{1313} = 1$ for $\lambda = 0$; with λ increased, C_{1313} and C_{2323} converge and for $\lambda = 10$ their difference falls between the statistical error margins.

Table 1. C_{1313} and C_{2323} of cracked solid as a function of crack density ρ and disorder parameter λ.

	$\lambda = 0$		$\lambda = 0.1$		$\lambda = 0.5$		$\lambda = 2$		$\lambda = 10$	
$\pi\rho$	C_{1313}	C_{2323}	C_{1313}	C_{2323}	C_{1313}	C_{2323}	C_{1313}	C_{2323}	C_{1313}	C_{2323}
0.5	1.0	0.640	0.962	0.655	0.880	0.706	0.803	0.770	0.783	0.784
1.0	1.0	0.432	0.926	0.460	0.772	0.525	0.643	0.602	0.633	0.633
1.5	1.0	0.323	0.885	0.341	0.678	0.405	0.535	0.481	0.516	0.515
2.0	1.0	0.243	0.848	0.267	0.600	0.328	0.472	0.415	0.442	0.433
2.5	1.0	0.188	0.811	0.212	0.559	0.289	0.416	0.367	0.369	0.375
3.0	1.0	0.150	0.737	0.176	0.501	0.237	0.375	0.324	0.344	0.342

Table 2. C_{1111} and C_{2222} of cracked solid as a function of crack density ρ and disorder parameter λ.

	$\lambda = 0$		$\lambda = 0.1$		$\lambda = 0.5$		$\lambda = 2$		$\lambda = 10$	
$\pi\rho$	C_{1111}	C_{2222}	C_{1111}	C_{2222}	C_{1111}	C_{2222}	C_{1111}	C_{2222}	C_{1111}	C_{2222}
0.5	2.792	1.132	2.570	1.192	2.112	1.379	1.757	1.600	1.674	1.663
1.0	2.718	0.509	2.294	0.540	1.542	0.680	1.067	0.912	0.993	0.990
1.5	2.693	0.266	2.051	0.285	1.117	0.384	0.699	0.570	0.636	0.609
2.0	2.682	0.137	1.824	0.153	0.854	0.223	0.486	0.355	0.413	0.414
2.5	2.677	0.084	1.642	0.094	0.670	0.148	0.346	0.258	0.301	0.295
3.0	2.672	0.046	1.492	0.071	0.530	0.113	0.267	0.195	0.218	0.217

Table 3. C_{1212} and C_{1122} of cracked solid as a function of crack density ρ and disorder parameter λ.

	$\lambda = 0$		$\lambda = 0.1$		$\lambda = 0.5$		$\lambda = 2$		$\lambda = 10$	
$\pi\rho$	C_{1212}	C_{1122}	C_{1212}	C_{1122}	C_{1212}	C_{1122}	C_{1212}	C_{1122}	C_{1212}	C_{1122}
0.5	0.700	0.377	0.692	0.357	0.690	0.327	0.688	0.306	0.685	0.298
1.0	0.498	0.158	0.494	0.132	0.480	0.068	0.478	0.043	0.477	0.040
1.5	0.373	0.080	0.360	0.046	0.344	-0.027	0.343	-0.053	0.341	-0.053
2.0	0.285	0.046	0.265	-0.007	0.258	-0.066	0.250	-0.096	0.252	-0.092
2.5	0.220	0.029	0.208	-0.033	0.196	-0.086	0.192	-0.096	0.195	-0.092
3.0	0.176	0.015	0.163	-0.021	0.158	-0.077	0.157	-0.086	0.155	-0.089

The analogous data for the components C_{1111}; C_{2222}; C_{1122} and C_{1212} of the effective stiffness tensor obtained from the plane strain problem are given in Table 2. Similarly to the previous example, C_{1111} and C_{2222} tend to each other with λ growing up. At the same time, as seen from Table 3, C_{1212} is only weakly affected by the disorder parameter λ. Another interesting feature is that in disordered structures, C_{1122} becomes negative starting from the crack density ρ=1.5/π.

The graphical illustration of the orientation factor effects is given in Fig. 2.

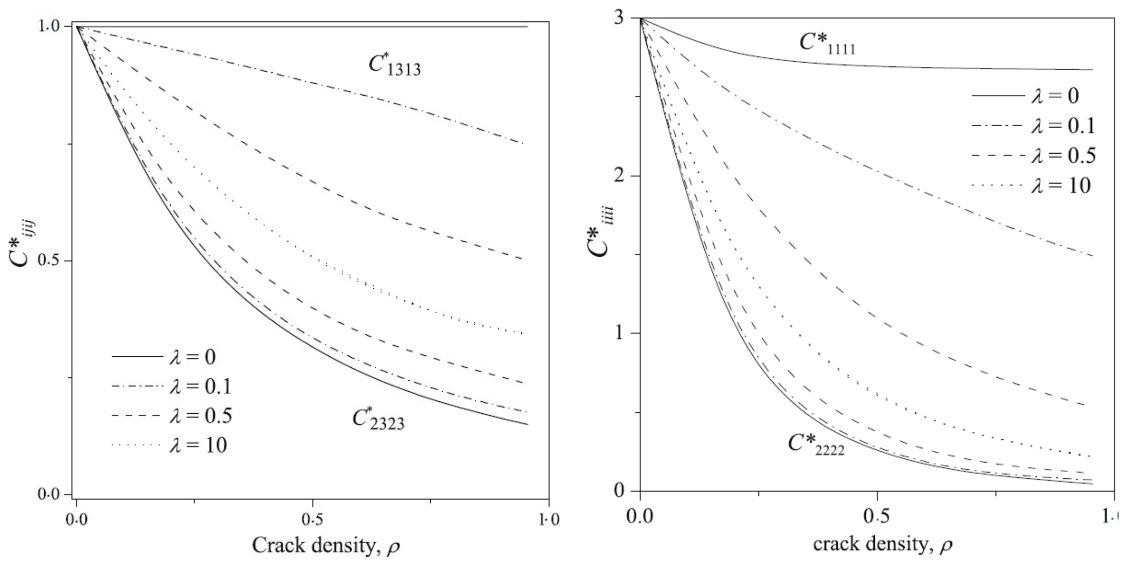

Fig. 2. Effective elastic anisotropy of cracked solid as a function of crack density ρ and disorder parameter λ.

2. Micro level model: effect of interface crack cluster formation on anisotropy of effective stiffness of composite

Publications:

1. V.I. Kushch, S.V. Shmegera, L. Mishnaevsky Jr (2008) Meso cell model of fiber reinforced composite: interface stress statistics and debonding paths. *International Journal of Solids and Structures* **45** 2758-2784.

2. V.I. Kushch, S.V. Shmegera, L. Mishnaevsky Jr (2009) Elastic interaction of partially debonded circular inclusions. I. Theoretical solution, accepted to *International Journal of Solids and Structures*

3. V.I. Kushch, S.V. Shmegera, L. Mishnaevsky Jr (2010) Elastic interaction of partially debonded circular inclusions. II. Application to fibrous composite, submitted to *International Journal of Solids and Structures*.

We consider the representative unit cell (RUC) model of fibrous composite. RUC model represents an infinite periodic structure, an elementary unit cell of which contains a certain number of inclusions: the whole volume of composite is obtained by replicating the cell in two orthogonal directions. To simulate progressive interface debonding in fiber reinforced composite, the cohesive-zone model of interface has been applied. This approach correctly predicts the main steps in interface crack cluster formation, see Fig. 3. Noteworthy, all the clusters are oriented across the loading direction.

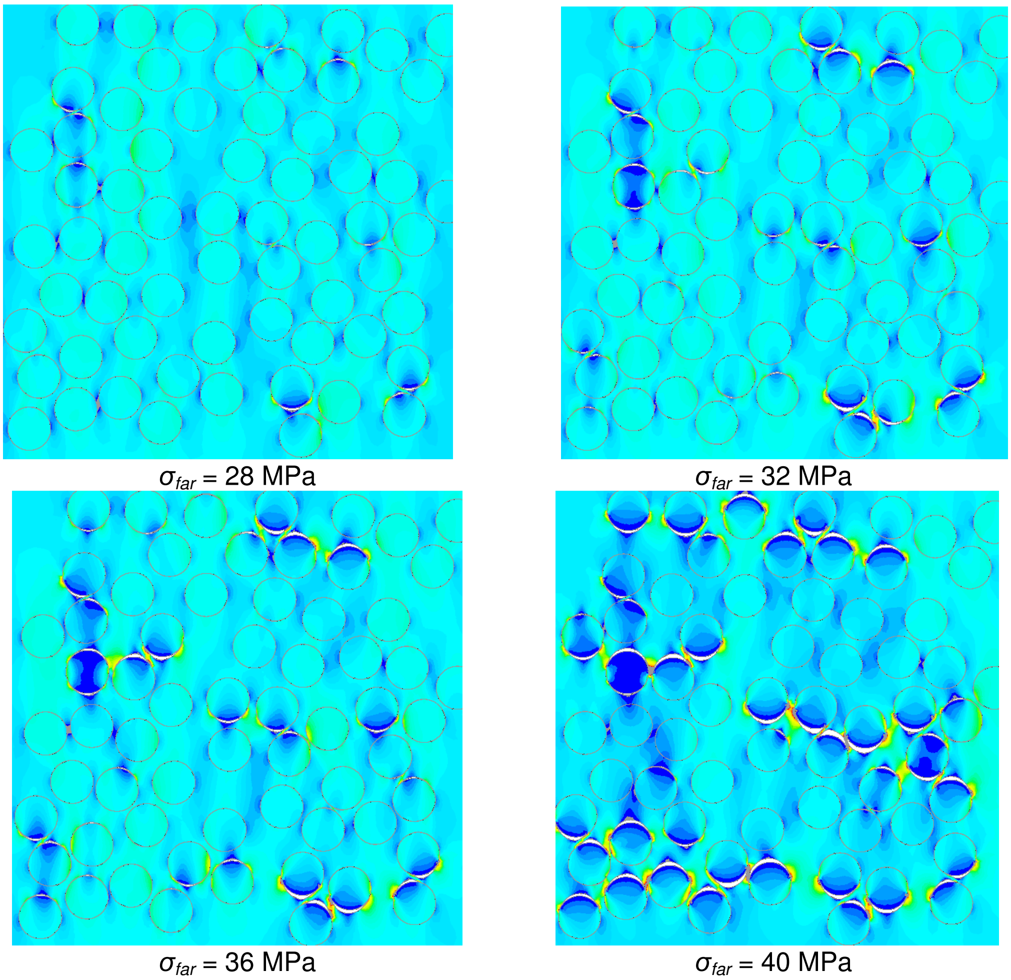

σ_{far} = 28 MPa | σ_{far} = 32 MPa

σ_{far} = 36 MPa | σ_{far} = 40 MPa

Fig 3. Interface debonding growth in a random structure FRC

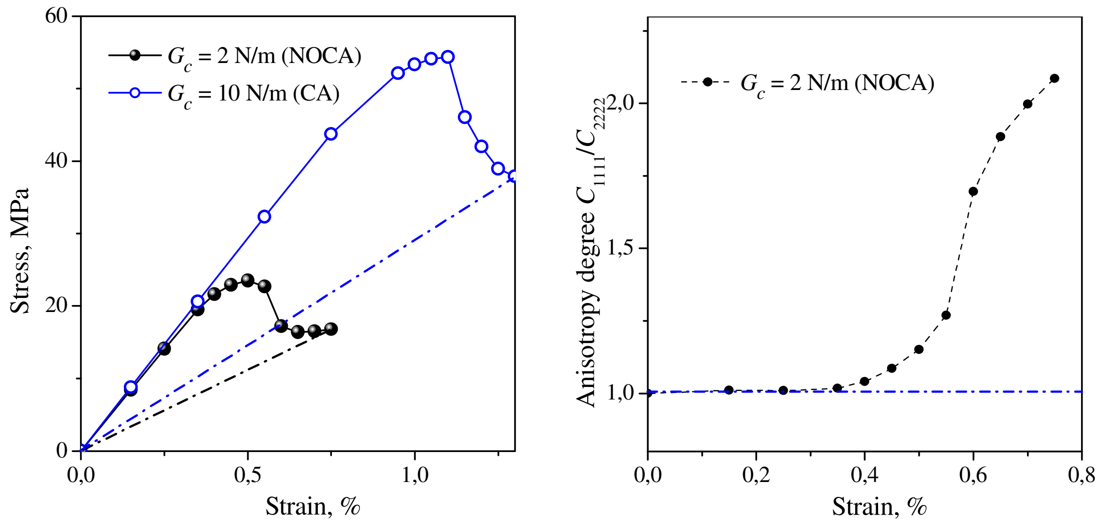

(a) (b)

Fig. 4. Elastic stiffness reduction and induced anisotropy due to interface debonding

The FRC stress-strain curves obtained from this model is shown in Fig. 4a. Noteworthy, matrix and fibers deform elastically so their non-linear behavior is entirely due to progressive interface damage. The irreversible strain does not accumulate: unloading is linearly-elastic, with reduced Young modulus (dash-dotted lines in Fig. 4a). Effective stiffness, strain-induced anisotropy and FRC strength limit can be estimated using these data. In Fig. 4b, an elastic stiffness anisotropy due to interface debonding is shown. As it would be expected, effective stiffness loss in x-direction is substantially lower than that one in y- (loading) direction.

3. Micro level model: effect of interface crack orientation on anisotropy of effective transverse conductivity of composite

Publications:

1. V.I. Kushch (2010) Transverse conductivity of unidirectional fibrous composite with interface arc cracks. *International Journal of Engineering Science* **48** 343–356.

A complete solution of the conductivity problem has been obtained for the finite and infinite arrays of circular inclusions with interface arc cracks regarded as the models of fibrous composite with interface damage. An exact and finite form expression of the effective conductivity tensor has been found by integrating the local fields over the representative cell volume. The numerical data given below discover the way and extent to which the conductivity of fibrous composite is affected by the interface debonding.

In Table 4, the components λ_{11} and λ_{22} of the effective conductivity tensor are given as the functions of the fiber volume content c and crack semi-length, θ_d. The preferably oriented cracks make the composite anisotropic, and caused by them reduction in conductivity is greater in x2-direction. For $\theta_d > \pi/3$; λ_{22} falls below the conductivity of a matrix material and, with c increased, an anisotropy degree grows rapidly.

Table 4. Effective conductivity as a function of *c* and θ_d.

c	$\theta_d = 0$		$\theta_d = \pi/6$		$\theta_d = \pi/3$		$\theta_d > \pi/2$	
	λ_{11}	λ_{22}	λ_{11}	λ_{22}	λ_{11}	λ_{22}	λ_{11}	λ_{22}
0.1	1.178	1.178	1.176	1.123	1.152	1.004	1.076	0.896
0.2	1.391	1.391	1.388	1.258	1.334	1.001	1.166	0.797
0.3	1.652	1.652	1.646	1.402	1.558	0.987	1.278	0.698
0.4	1.981	1.981	1.974	1.550	1.850	0.957	1.430	0.596
0.5	2.415	2.415	2.409	1.696	2.248	0.909	1.650	0.489
0.6	3.037	3.037	3.032	1.838	2.838	0.843	1.998	0.373
0.7	4.062	4.062	4.058	1.989	3.843	0.762	2.662	0.236

The curves in Fig. 5 illustrate an effect of crack orientation with respect to the major lattice axes. This effect is more pronounced in high-filled composite. Also, in this case the skew component k_{12} is non-zero as well, see Fig. 5b.

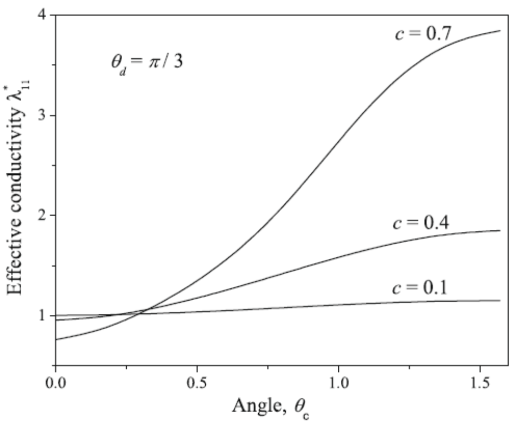

(a)

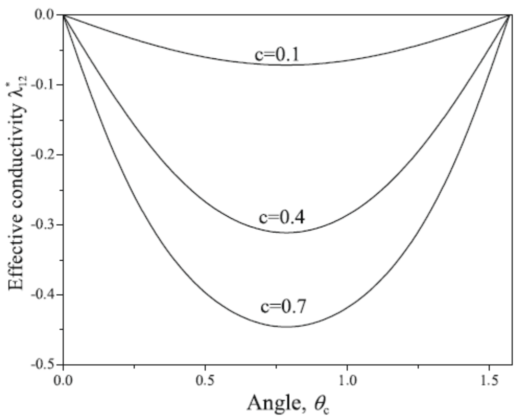

(b)

Fig. 5. Anisotropy of effective conductivity: an effect of arc crack orientation

4. Macro level model: effective stiffness of aligned fiber reinforced composite with anisotropic constituents

Publications:

1. V.I. Kushch, I. Sevostianov, L. Mishnaevsky Jr (2008) Stress concentration and effective stiffness of aligned fiber reinforced composite with anisotropic constituents. *International Journal of Solids and Structures* **45** 5103–5117.

As was shown above, during the service life the damage-induced anisotropy of FRC constituents is developing due to the preferably oriented micro cracks growth in the components or due to partial debonding along the matrix-fibers interface. This effect must be taken into consideration in the macro-level model aimed to calculate the local stress field and effective elastic properties of a unidirectional fiber reinforced composite with anisotropic constituents. To analyze this model, an accurate analytical method and relevant applied software has been developed. The model enables evaluation of the damage induced anisotropy in terms of the averaged properties of damaged components.
An effect of phase anisotropy is seen from the reported below numerical data obtained for $C^-_{44} = 10$; $C^-_{55} = 1$; $C^-_{45} = 0$; the local stress corresponds to the macroscopic anti-plane shear $E_{23} = 1$. In Table 5, the components C^*_{44} and C^*_{55} of the effective stiffness tensor are given and a function of volume fraction of the fibers, assumed here to be elastically isotropic. It is seen from the table that the absolute values of effective moduli as well as the effective anisotropy degree can vary widely depending on the structure parameters of composites.

Table 5. Effective elastic moduli C^*_{44} and C^*_{55} as a function of c and C^+

c	$C^+ = 0$		$C^+ = 2$		$C^+ = 10$		$C^+ = 1000$	
	C^*_{55}	C^*_{44}	C^*_{55}	C^*_{44}	C^*_{55}	C^*_{44}	C^*_{55}	C^*_{44}
0.1	0.862	7.329	1.078	8.399	1.259	10.0	1.363	11.58
0.2	0.723	5.776	1.157	7.243	1.519	10.0	1.729	13.76
0.3	0.590	4.592	1.238	6.291	1.815	10.0	2.173	16.79
0.4	0.467	3.598	1.323	5.464	2.176	10.0	2.771	21.09
0.5	0.353	2.723	1.415	4.720	2.645	10.0	3.657	27.63
0.6	0.247	1.923	1.514	4.035	3.295	10.0	5.169	38.93
0.7	0.141	1.136	1.623	3.384	4.312	10.0	8.705	65.37

On one hand, it makes prediction of their elastic behavior a rather complicated problem and justifies development and application for their study of the accurate methods. On the other hand, high structural sensitivity opens a wide opportunity for solving the optimization problems, i.e., designing the composites with a required set of mechanical properties by a proper combination of anisotropic constituents. The developed analytical method is sufficiently flexible and efficient to provide substantial progress in solving the problems of this kind.